BJES Basrah Journal for Engineering Sciences

Basrah Journal for Engineering Sciences, Vol. 21, No. 1, (2021), 20-26

Original Article

Journal homepage: www.bjes.edu.iq
ISSN (Online): 23118385, ISSN (Print): 18146120

OPEN ACCESS

Flexible rotor balancing without trial runs using experimentally tuned FE based rotor model

Yahya Muhammed Ameen [1,*], Jaafar Khalaf Ali [2]

[1,2,3]*Department of Mechanical Engineering, College of Engineering, University of Basrah, Basrah, Iraq*
E-mail addresses: yahyaameen@yahoo.com , jaafarkhalaf@yahoo.com
Received: 1 July 2020; Accepted: 4 August 2020; Published: 17 January 2021

Abstract

A method based on experimentally calibrated rotor model is proposed in this work for unbalance identification of flexible rotors without trial runs. Influence coefficient balancing method especially when applied to flexible rotors is disadvantaged by its low efficiency and lengthy procedure, whilst the proposed method has the advantage of being efficient, applicable to multi-operating spin speeds and do not need trial runs. An accurate model for the rotor and its supports based on rotordynamics and finite elements analysis combined with experimental modal analysis, is produced to identify the unbalance distribution on the rotor. To create digital model of the rotor, frequency response functions (FRFs) are determined from excitation and response data, and then modal parameters (natural frequencies and mode shapes) are extracted and compared with experimental analogies. Unbalance response is measured traditionally on rotor supports, in this work the response measured from rotating disks instead. The obtained results show that the proposed approach provides an effective alternative in rotor balancing. Increasing the number of balancing disks on balancing quality is investigated as well.

Keywords: Flexible rotor, Balancing, Unbalance identification, Finite elements, Experimental modal analysis, Rotordynamics.

http://dx.doi.org/10.33971/bjes.21.1.4

1. Introduction

Rotor unbalance is the main cause of rotor vibration and its serious consequences. When such problems met, it is resorted to balancing process, which includes attaching correction masses in predefined balancing planes to compensate eccentric mass distribution that generates large centrifugal forces and the high levels of vibration. Determining the magnitude, phase (angular position) and axial distribution of the correction masses along the shaft, is the objective of the balancing process.

Mostly, if the rotational speed of the rotor approximates or exceeds its critical speed, the resulting vibrations due to unbalance become serious. This is a result of considerable deflections in the rotor when operating in the vicinity of its critical speed.

When the rotor operates below 70 % of its critical speed, it is known as rigid rotor. This type when balanced at one speed will be balanced at any speed below 70 % of its critical speed. In contrary, flexible rotor (that operates above 70 % of its critical speed) will distort due to unbalance (centrifugal) forces, and when balanced at one speed, may not be balanced at another speed.

Two main strategies still in use widely until now, are influence coefficients method and modal balancing method. The influence coefficients method assumes direct and linear proportion between the unbalance (cause) and the measured response (effect) of the rotor, and can be employed to balance rigid and flexible rotors. Modal Balancing method aims to balance flexible rotor using its modal properties. In this technique, every vibration mode was corrected by attaching a set of masses to the rotor so that no effect was caused on previously balanced modes.

Both two techniques have its own advantages and disadvantages, but the common feature of the two is the large number of trial runs required to identify the correction masses (in the literature, several texts and papers give exhaustive description [1, 2]). Modal balancing method cannot be adopted in this work for the following reasons:

1. Restricted optionality in selecting the axial locations of balancing planes, since the rotor under study is relatively short and considerable spaces on its length are occupied by coupling, supports and shaft collars on the discs. Hence available spaces for the discs will be limited.
2. In a system with influential damping as in the rotor under study, the mode shapes do not appear clearly.

On the other hand, efficiency of influence coefficients method depends highly on number of trial runs, which are cost and time consuming and even may expose the rotor parts to damage. Thus, it is required to minimize or eliminate the trial runs. In this work, the rotor taken as a balancing case study will be described (physically in detail in the following sections), and examined at 70 %, 83 %, 92 % and 140 % of the first critical rotational speed, and thus it is considered as flexible rotor. This wide and "critical speed crossing" range of operational speeds, makes the influence coefficients method not applicable in its traditional strategy [2].

The alternative is the balancing procedure proposed in this work, which is Model Based Balancing (MBB) method. The model in MBB is digital twin to the real rotor [3]. One of the most important features of the MBB is the reduction of

required trial runs (i.e., costs and efforts) of the balancing procedures to identify the correction masses. Accurate mathematical simulation of the machine (especially rotor bearings and foundation assembly) is the cornerstone in MBB. Such approach solves inverse dynamical problems for rotating machinery [4], and by taking into account the uncertain parameters of the rotor that can affect the balancing result [13].

Various contributions have been presented based on mathematical model of the rotor system. Carvalho et al. [13] proposed an approach based on mono-objective optimization solution of mathematical model, taking unbalance contribution along the rotor as uncertain information. Considerable unbalance reduction was achieved, although mode shapes are not taken in account, and trial weights are required. Yun et al. [14] developed an online balancing method based on dynamic influence coefficients matrix and FE model, without trial runs. However, the method was applied on rigid rotor with single balancing plane. Siegl and Markert [15] overcame the limitations concerning speed dependency, mainly met in balancing methods, as they demonstrate experimentally a time-domain algorithm for model-based unbalance identification. However, in addition to the requirement of single run, their method is applicable on limited types of rotors.

The desired accurate model is not easily created, and generally the following issues should be dealt with:

1. Mutual effects between rotor shaft and its carried disks on the one hand, and rotor support (bearings, pedestals … etc.) on the other hand.
2. Exact geometrical and mathematical simulation of the (especially industrial) rotor parts.
3. Obtaining the actual and accurate values of mechanical properties (density, Young's modulus, Poison's ratio, stiffness, damping … etc.) for rotor parts.

To facilitate this task, it is suggested in this work that the required model can be attained by the following briefly explained steps:

1. Perform the Experimental Modal Analysis (EMA) on the rotor under balancing test, and extract its fundamental natural frequencies and mode shapes.
2. Within reasonable accuracy limits, build the twin digital model. For this purpose, Finite Element Analysis (FEA) is the best tool. Again, as in previous step calculate the significant natural frequencies and mode shapes.
3. Compare the experimentally and analytically resulting natural frequencies and mode shapes. In this stage differences are usual and expected, and can be minimized acceptably by changing (tuning) the values of the changeable and effective parameters in the mathematical model.

Within the selected frequency range in step 1 above, it is expected that resulting digital model behaves dynamically similar to its real twin. Hence, trial runs can be done digitally to find the required influence coefficients, leading to find the unbalance distribution from measured response.

2. Balancing Test Rig

Machinery Fault Simulator shown in Figure 1 is used in this work to perform flexible rotor balancing and to verify the efficiency of the MBB and the proposed procedure. The rotor consists of 0.5" diameter solid structural steel shaft of 550 mm length, carrying 3 identical structural steel disks, as in schematic diagram in Figure 2. The rotor is attached by Aluminum flexible coupling to speed-controlled motor, and supported by two deep groove ball bearings.

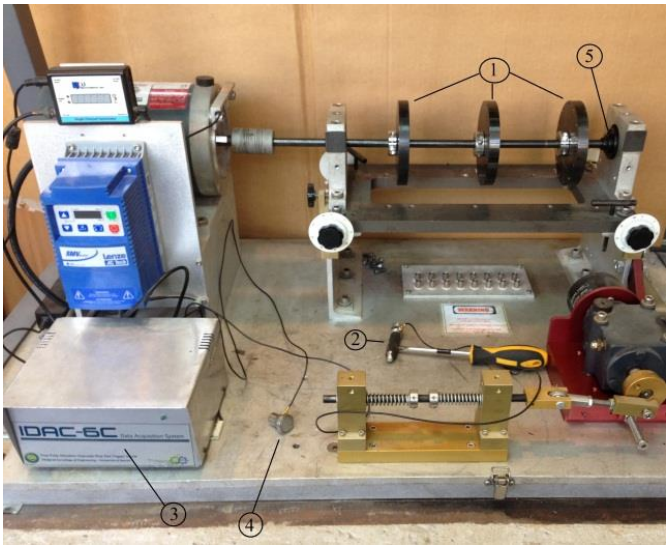

1. Disks, 2. Impact Hammer, 3. Data acquisition system, 4. Accelerometer, 5. Ball bearing.

Fig. 1 Machinery Fault Simulator used as balancing test rig.

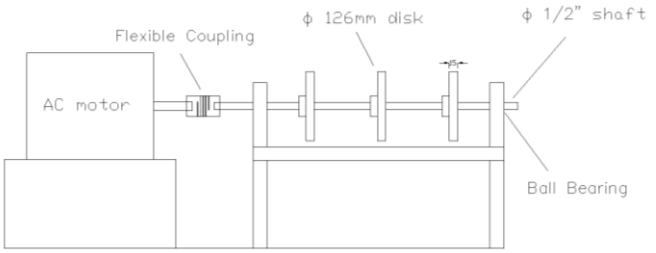

Fig. 2 Schematic diagram of the rotor.

3. Experimental Modal Analysis (EMA)

Measuring both the external force applied to the structure and resulting response, leads to deduction of frequency response functions (FRF) and then modal parameters (natural frequencies, mode shapes and modal damping factors). This is the principle idea of experimental modal analysis or modal testing. EMA consider linear and time invariant systems. In this section we will present only the main principles of EMA and related excitation techniques.

The equation of motion of viscously damped forced multi degree of freedom system is given by [5]:

$$\boldsymbol{M}\{\ddot{x}\} + \boldsymbol{C}\{\dot{x}\} + \boldsymbol{K}\{x\} = \{f(t)\} \tag{1}$$

Where $x(t)$ describing the displacement due to the applied force $f(t)$, $\boldsymbol{M}$ is the mass matrix, $\boldsymbol{C}$ is the damping matrix, and $\boldsymbol{K}$ is the stiffness matrix. The Laplace transform of the above equation is:

$$[\boldsymbol{M}s^2 + \boldsymbol{C}s + \boldsymbol{K}]\{\boldsymbol{X}(s)\} = \{\boldsymbol{F}(s)\} \tag{2}$$

The dynamic stiffness matrix is $\boldsymbol{Z}(s) = [\boldsymbol{M}s^2 + \boldsymbol{C}s + \boldsymbol{K}]$

Receptance matrix is

$$\boldsymbol{\alpha}(s) = \frac{\{\boldsymbol{X}(s)\}}{\{\boldsymbol{F}(s)\}} = \boldsymbol{Z}(s)^{-1} = [\boldsymbol{M}s^2 + \boldsymbol{C}s + \boldsymbol{K}]^{-1}$$

$$\{\boldsymbol{X}(s)\} = \boldsymbol{\alpha}(s)\,\{\boldsymbol{F}(s)\} = \begin{bmatrix} \alpha_{11}(s) & \alpha_{12}(s) & \cdots \\ \alpha_{21}(s) & \alpha_{22}(s) & \cdots \\ \vdots & \vdots & \ddots \end{bmatrix} \{\boldsymbol{F}(s)\} \quad (3)$$

Where $\alpha_{ij}(s)$ relates the response at node *i* with the only force at node *j*.

$$\alpha(s) = [\boldsymbol{M}s^2 + \boldsymbol{C}s + \boldsymbol{K}]^{-1} = \frac{adj(\boldsymbol{M}s^2 + \boldsymbol{C}s + \boldsymbol{K})}{det(\boldsymbol{M}s^2 + \boldsymbol{C}s + \boldsymbol{K})} \quad (4)$$

When the damping is small, the roots of the characteristic polynomial equation in the numerator are complex conjugate pole pairs, λ_r and λ_r^* , r = 1, 2, …, N, with N the number of modes of the system. The transfer function can be rewritten in a pole-residue form or the so-called "modal" model (assuming all poles have multiplicity one):

$$\alpha(s) = \sum_{r=1}^{N} \left(\frac{R_r}{s - \lambda_r} + \frac{R_r^*}{s - \lambda_r^*} \right) \quad (5)$$

The residue matrices R_r are given by:

$$R_r = \lim_{s \to \lambda_r} (\alpha(s)(s - \lambda_r)) \quad (6)$$

With

$$\alpha_{ij}(s) = \sum_{r=1}^{N} \left(\frac{{}_rR_{ij}}{s - \lambda_r} + \frac{{}_rR_{ij}^*}{s - \lambda_r^*} \right) \quad (7)$$

The elements of FRF are found by letting s = jω (when displacement is the response parameter, FRF is called a "Receptance FRF" and is usually written as $\alpha(\omega)$):

$$\alpha_{ij}(j\omega) = \sum_{r=1}^{N} \left(\frac{{}_rR_{ij}}{j\omega - \lambda_r} + \frac{{}_rR_{ij}^*}{j\omega - \lambda_r^*} \right) \quad (8)$$

The equivalent non-factorized (polynomial) form is given by:

$$\alpha_{ij}(j\omega) = \sum_{r=1}^{N} \frac{{}_rA_{ij}}{\omega_r^2 - \omega^2 + 2j\zeta\omega\,\omega_r} = \sum_{r=1}^{N} \frac{\phi_{ir}\,\phi_{jr}}{\omega_r^2 - \omega^2 + 2j\zeta\omega\,\omega_r} \quad (9)$$

$$A_r = \begin{Bmatrix} \phi_1 \\ \phi_2 \\ \vdots \\ \phi_N \end{Bmatrix}_m \lfloor \phi_1 \quad \phi_2 \quad \dots \quad \phi_N \rfloor_m \quad (10)$$

Where $\phi_1, \phi_2, \dots \phi_N$ are modal constants. These are scaled (or mass-normalized) modal constants. In experimental modal analysis, modal constants ${}_rA_{ij}$ are estimated from the measured FRF data.

Here λ_m is the complex frequency (Eigen value) of the m^{th} mode:

$$\lambda_r = -\zeta_r\,\omega_r + j\sqrt{1 - \zeta_r^2}\;\omega_r = \sigma_r + j\omega_{d,r} \quad (11)$$

with $f_d = \omega_d/2\pi$ the damped natural frequency,

$f_n = \omega_n/2\pi$ the (undamped) natural frequency

Where, $\omega_n = |\lambda|$, and $\zeta = c/2m\omega_n = \sigma/|\lambda|$ the damping ratio ($f_d = f_n\sqrt{1-\zeta^2}$).

Commonly, there are two ways to apply excitation force on tested structure:

3.1. Impact Hammer

Used to excite the structure by impulse force. Ideal Impact means ideal impulse force, which is in turn motivate largest number of vibrational modes with equal energy.

Force sensor is fixed to the end of the impact hammer to measure and record the force. Hard tip is fitted to the hammer used in this work to excite wider range of frequencies. Brüel and Kjaer type 8200 force transducer is used to collect impact force data, while Brüel and Kjaer type 4366 with mass of 26 g vibration transducer (piezoelectric accelerometer) is used to collect the dynamic response data (hence, it is so called "Instrumented Hammer"). The frequency response function was generated at a host notebook computer using SigTool software. Modal parameters are extracted from generated FRFs using MEscope software, utilizing its MDOF curve-fitting tool.

3.2. Shaker

It is electrical device used as source of force to excite the structure at single point as impact hammer do. Prepared and amplified input signal (sinusoidal, sweep-sine, or random signal in a specified frequency band) fed to shaker.

4. Influence Coefficients Balancing Method

In this method influence coefficient relates linearly input to output. Where input is an unbalance force (U) acting in one of the balancing (compensation) planes *k*, and an output is a response at one degree of freedom, for example a relative displacement (*x*).

Fig. 3, shows 3D drawing of rotor with three compensation planes (disks), selected and fabricated in such a manner that compensation weights can be attached, and the unbalance response can be measured at any of them (although, vibrations are measured at bearing locations in most cases).

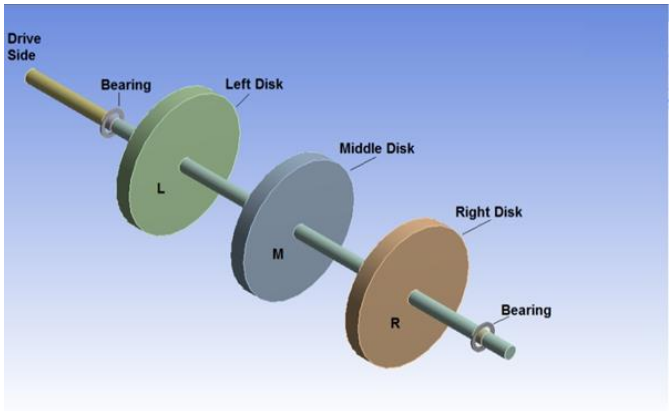

Fig. 3 Example of 3-Disk rotor.

Vibration in rotating structures, is a function of inherent parameters of the system (mass, damping, stiffness) and excitation parameters (e.g. unbalance), which are together influence this vibration [3]. To solve this problem, it is often referred to influence coefficients balancing, the well-known and recommendable strategy.

Influence coefficient (α_{ik}) can be determined experimentally by applying trial mass U_k in the balancing plane k and measuring the response (may be displacement, velocity or acceleration) x_i at the degree of freedom i:

$$x_{ik} = X_{ik} - X_i^o \tag{12}$$

Where, X_{ik} is the response in plane i due to applying trial mass in plane k, and X_i^o is the initial (as found) response in plane i. Then

$$\alpha_{ik}(\Omega) = \frac{x_{ik}(\Omega)}{U_k} = \alpha_{ik\,Re} + j\,\alpha_{ik\,Im} \tag{13}$$

Equation (13), shows that the influence coefficient α_{ik} relates linearly the unbalance U_k (cause) at plane k, with the measured response x_i (effect) at the plane i. Worth mentioning that, if it is allowed practically, the same plane can be used for applying balancing weights and response measuring. Influence coefficients values are functions of rotor rotational speed and dynamic properties of the rotor and its supporting structure as well. Since both unbalance and measured responses have magnitude and phase angle, they are represented as complex numbers, and thus influence coefficients are complex numbers.

The dimensions of the matrix of influence coefficients depend on the number of response measurements and the number of balancing planes. In the example shown in Fig. 3, three balancing planes (L, M and R) and two response measurement planes (L and R). Therefore, the influence coefficients matrix contains 6 influence coefficients describe the relation between three unbalances and two measured displacements, as in equation (14) below:

$$\begin{bmatrix} x_L \\ x_R \end{bmatrix} = \begin{bmatrix} \alpha_{LL} & \alpha_{LM} & \alpha_{LR} \\ \alpha_{RL} & \alpha_{RM} & \alpha_{RR} \end{bmatrix} \begin{bmatrix} U_L \\ U_M \\ U_R \end{bmatrix} \tag{14}$$

As mentioned in the introduction, determining the influence coefficients experimentally can be very time consuming. However, in this work, the reliable Finite Element Analysis (FEA) software ANSYS workbench 15, together with FEA MATLAB code [6] are utilized to consider all the effective parameters to create reliable numerical model of the rotor.

5. Results and Discussion

Two case studies will be extracted and discussed in this work:

1. Two measuring planes (L and R disks) and two balancing planes (L and R disks).
2. Two measuring planes (L and R disks) and three balancing planes (L, M and R disks).

Digital model of the rotor is common for both case studies, and should be available in advance to calculate influence coefficients matrix. The three suggested steps in the introduction are carried out as following:

5.1. Experimental Modal Analysis (Modal Testing)

Selecting suspending method and proper number and locations of impact points is principal step in modal testing [12]. Increasing the number of impact points is advantageous [7] specially to obtain accurate mode shapes. However, it is supposed that nine points are adequate because:

1. It is aimed in this work to extract two fundamental mode shapes. Higher mode shapes require larger number of points to be well described.
2. Against increasing the number of impact points, practical limitation arises due to small available length of the shaft. Total length of the shaft is 550 mm, but when subtracting the length occupied by disks, supports and coupling, remaining available length is less than 400 mm.

These impact points, as shown in Fig. 4, are unevenly distributed to avoid impacting on the disks, supports and coupling.

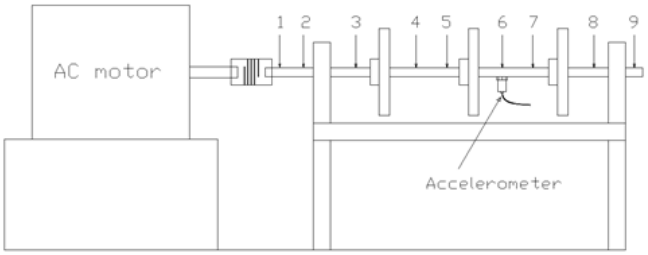

Fig. 4 Impact points.

Overlaid FRFs resulting from impacting and measuring response (acceleration) horizontally and vertically are shown in Figs. 4(a) and 4(b) respectively.

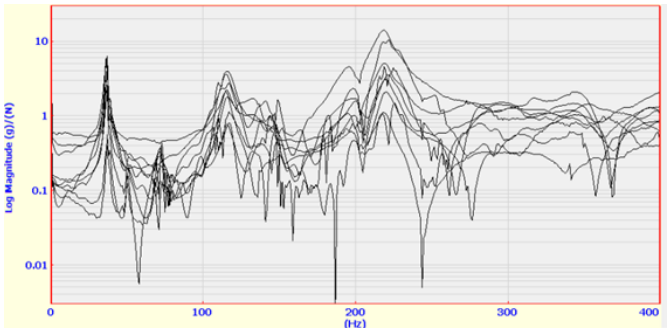

(a)

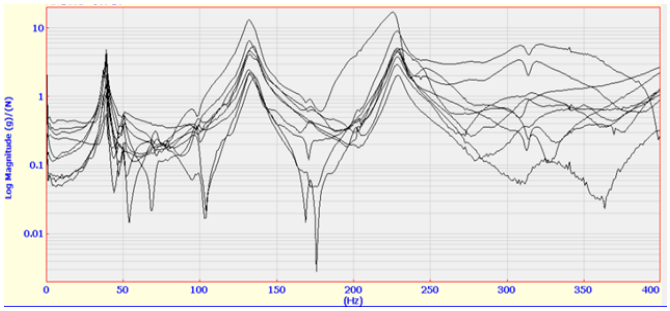

(b)

Fig. 5 FRFs resulting from (a) Horizontal impact and response (b) Vertical impact and response.

Table 1 shows the fundamental natural frequencies and mode shapes resulting from modal testing. It is aimed in this work to examine MBB in rotational speed range of 1500 rpm (25 Hz) to 3000 rpm (50 Hz). Hence, values of natural frequencies shown in Table 1 support the decision of satisfaction by two fundamental modes.

Table 1 Fundamental natural frequencies and mode shapes from modal testing.

	First Mode	Second Mode	Third Mode
Horizontal Vibration	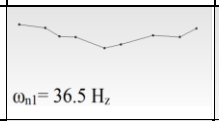	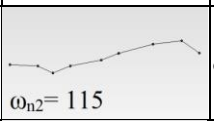	**ωn3 = 220 Hz**
Vertical Vibration	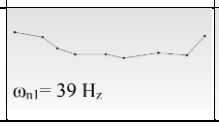	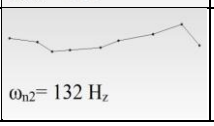	**ωn3 = 228 Hz**

5.2. Finite Elements Based Model

Building this model can be achieved by two ways: ANSYS Workbench software or MATLAB code. It is experienced by the researchers in this work that modal parameters (natural frequencies and mode shapes) when extracted from the two ways, differences in results are not significant. Table 2 shows ANSYS results of the elementary model of the rotor, in which materials properties and solution settings are as in the software defaults, and ball bearings stiffness in the two principal directions are assumed initially as recommended values in literature [8], with no damping.

Table 2 Fundamental natural frequencies and mode shapes from ANSYS FEA software.

	First Mode	Second Mode	Third Mode
Horizontal Vibration	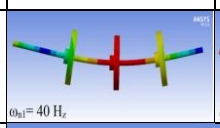	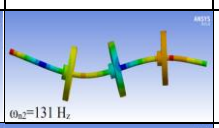	**ωn3 = 252 Hz**
Vertical Vibration	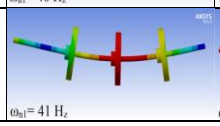	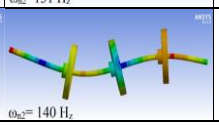	**ωn3 = 265 Hz**

5.3. Comparison of the Resulting Modal Parameters

Although mode shapes identification is not required in the influence coefficients calculations, it might be used as an important criterion to qualify the suitability of the digital model of the rotor. Mode shapes extracted from modal testing Table 1 and FEA Table 2 show obvious similarity.

Significant differences seen in natural frequencies obtained experimentally and theoretically, thus minimizing this error is needed. In this stage, dynamic properties of the rotor supports are the most changeable and effective parameters that affect dynamic behavior of the rotor, and expected to adjust natural frequencies as wanted. The following remarks should be noticed:

1. Tables 1 and 2 show that theoretical values of natural frequencies are larger than analogous experimental. The task is to reduce theoretical values until acceptable difference is reached. Among many parameters, the most effective should be employed. The researcher should be able to expect the relation (direct or inverse) of these parameters with natural frequencies.
2. In ANSYS software, stiffness and damping properties of the bearing and its support of the real rotor may be merged to find equivalent (overall) stiffness and damping and then tuned. In spite of isotropic dynamic properties of the deep groove ball bearings, the supporting structure has generally anisotropic dynamic properties, leading to anisotropic equivalent stiffness and damping. The rotor in this this work has relatively simple design structure, so it is easy to deduce that horizontal stiffness less than vertical.
3. Changing any one of the effective parameters in the mathematical model will certainly change irregularly (increase or decrease) natural frequencies of all modes.

Accordingly, engineering insight is crucial to create the digital model of the rotor.

In Table 3, final results after taking in consideration above remarks. Mode shapes are not included in this table, since they are not needful in this stage, and the range of carried out tuning has no significant effect on them.

Table 3 Natural frequencies [Hz]: Experimental and final (tuned) theoretical results.

	First Mode		Second Mode		Third Mode	
	Horizontal	**Vertical**	**Horizontal**	**Vertical**	**Horizontal**	**Vertical**
Experimental (Modal Testing)	36.5	39	115	132	220	228
Theoretical (FEA)	36	37	108	120	186	209
Difference [%]	1	5	6	9	15	8

As mentioned in the remark (2) above, the fact that horizontal stiffness of the two supports is less than vertical, leads to conclude that horizontal response (displacement) due to unbalance will be greater than vertical for the same point on the rotor shaft axis, i.e. forming horizontal elliptical orbit. Hence during tuning, priority was given to correct the natural frequencies of horizontal modes to be nearer to the experimental results. It is deemed that the results listed in Table 3 are acceptable to progress in MBB procedure.

5.4. Case Studies

Now, the required digital model is in hands, and ready to apply on the following two cases. The difference between the two cases is the number of balancing disks. Knowing that the first critical speed is 36 Hz, it is decided to examine the MBB at four rotational speeds: 25 Hz, 30 Hz, 33 Hz and 50 Hz, with about 70 %, 83 %, 92 % and 140 % of the first critical speed, respectively.

Case I: Two measuring planes and two balancing planes:

In this case left and right discs are considered as balancing and response measuring planes in the same time, while middle disc has no contribution.

As found (recorded prior to balancing) horizontal displacement response measured from the two discs at the selected four rotor speeds using non-contact linear displacement sensor.

Assuming the responses at left and right plane are due to unbalance masses at left and right disks and only, the following equation can be written:

$$\begin{Bmatrix} X_{1L} \\ X_{1R} \end{Bmatrix} = -\begin{bmatrix} \alpha_{LL} & \alpha_{LR} \\ \alpha_{RL} & \alpha_{RR} \end{bmatrix} \begin{Bmatrix} W_L \\ W_R \end{Bmatrix} \tag{15}$$

Where the coefficients α_{LL}, α_{LR}, α_{RL} and α_{RR} are obtained from the receptance matrix of the digital model at the specified rotational speed. Numerical values of these coefficients at 25 Hz are found to be as:

$$\begin{bmatrix}\alpha_{LL} & \alpha_{LR}\\ \alpha_{RL} & \alpha_{RR}\end{bmatrix} = \begin{bmatrix}-1.439-0.02593i & -2.248+0.0003500i\\ -2.254+0.0008570i & -1.313-0.02028i\end{bmatrix}\times 10^{-2} \quad (16)$$

Unknowns (WL and WR) in equation (15) can be calculated analytically. However, MATLAB code written for FEA of rotors [6] is modified here to perform rotor modeling and calculating the correction weights. In this code, rotational speed and measured response (magnitude and phase) in the two planes are the input data, while magnitude and attachment angle of correction masses are the output. Table 4 lists the vibration amplitudes before balancing and after applying described proposed balancing procedure.

Case II: Two measuring planes and three balancing planes:

Middle disc (M) in this case will be utilized as balancing plane likely to left and right discs, and no longer is idle. Receptance coefficients matrix in this case will be (2 × 3):

Table 4 Vibration amplitudes in case of two balancing planes and two measurement planes.

Rotational Speed [Hz]	**25**		**30**		**33**		**50**	
Plane	**L**	**R**	**L**	**R**	**L**	**R**	**L**	**R**
Initial vibration [mm]	0.1014	0.1109	0.2049	0.2239	0.4132	0.4719	0.2	0.2051
Vibration after balancing [mm]	0.0348	0.0495	0.0554	0.0784	0.0906	0.1498	0.0644	0.0448
Correction mass [g]	2.24 @152.5°	2.75 @95.4°	1.8 @143.7°	2.51 @92.3°	1.15 @189°	3.35 @90.9°	1.61 @66.1°	1.74 @94.2°
Vibration Reduction [%]	66	55	73	65	78	68	68	78

Table 5 Vibration amplitudes in case of three balancing planes and two measurement planes.

Rotational Speed [Hz]	**25**			**30**			**33**			**50**		
Plane	**L**	**M**	**R**	**L**	**M**	**R**	**L**	**M**	**R**	**L**	**M**	**R**
Initial vibration [mm]	0.1014		0.1109	0.2049		0.2239	0.4132		0.4719	0.2		0.2051
Vibration after balancing [mm]	0.0330		0.0505	0.0844		0.0978	0.1745		0.1401	0.0842		0.0780
Correction mass [g]	1.37 @179.6°	1.55 @121.0°	1.77 @78.8°	1.02 @175.1°	1.37 @113.6°	1.58 @78.2°	1.32 @232.4°	1.18 @110.8°	2.52 @83.8°	0.72 @46.5°	1.13 @80.4°	0.85 @109.4°
Vibration Reduction [%]	67		54	59		56	58		70	58		62

$$\begin{Bmatrix}X_{1L}\\ X_{1R}\end{Bmatrix} = -\begin{bmatrix}\alpha_{LL} & \alpha_{LM} & \alpha_{LR}\\ \alpha_{RL} & \alpha_{RM} & \alpha_{RR}\end{bmatrix}\begin{Bmatrix}W_L\\ W_M\\ W_R\end{Bmatrix} \quad (17)$$

The six elements of matrix in equation (17) can be obtained from the receptance matrix of the model at the specified rotor speed considering three balancing planes and two measuring planes. Numerical values of these coefficients at 25 Hz are found to be as:

$$\begin{bmatrix}\alpha_{LL} & \alpha_{LM} & \alpha_{LR}\\ \alpha_{RL} & \alpha_{RM} & \alpha_{RR}\end{bmatrix} = \begin{bmatrix}-1.439-0.02593i & -3.110-0.03023i & -2.248+0.0003500i\\ -2.254+0.0008570i & -3.023-0.02306i & -1.313-0.02028i\end{bmatrix}\times 10^{-2} \quad (18)$$

Results of applying correction masses on three planes are listed in Table 5.

6. Conclusions

To perform flexible rotor balancing, Model-Based Balancing (MBB) method supported by Experimental Modal Analysis (EMA) and Finite Element Analysis (FEA) is used in this work, and proper correction masses are found. Thus, disadvantages of multiple trial runs to calculate the influence coefficients are overstepped. Results obtained are promising and show very good vibration reduction, making this method acceptable for practical applications.

Effects of increasing the number of balancing planes (disks) from two to three are examined. Results show that no significant effects of this increase on balancing quality.

Separation in FRFs peaks has been shown at high frequencies (higher modes). The main reason is the presence of noise, where results show that lower signal/noise results from very low or very high rotational speeds, leading to deterioration in vibration measurement and FRFs quality. It is remarkable that among balancing speeds (25 Hz, 30 Hz, 33 Hz, and 50 Hz), optimum results are found at the 33 Hz, although

this speed is the nearest (92 %) to first critical speed, which is a result of the higher vibration signal/noise ratio, and precise tuned mathematical model of the rotor.

In rotor balancing, practical limitations may be encountered when measuring vibration response on supports (bearings planes), and the alternative is utilizing balancing planes instead. In the cases studied in this work, unbalance vibration responses are acquired from balancing planes. Nevertheless, the proposed method showed very good balancing quality.

7. Recommendations

1. Deep groove ball bearings are used in the rotor under study. It is useful to examine the proposed method on other types of bearings.
2. Estimation of accurate influence coefficients depends on the modal parameters resulting from EMA, which is applied in this work on stationary rotor. However, when EMA is applied on the rotor when it is under rotation [10,11], best results may be obtained.

References

[1] F. Ehrich, Handbook of Rotordynamics, McGraw – Hill, 1992.

[2] M. S. Darlow, Balancing of High-Speed Machinery, Springer-Verlag, 1989.

[3] R. Nordmann, E. Knopf and B. Abrate, "Numerical Analysis of Influence Coefficients for on Site Balancing of Flexible Rotors", Proc. of the 10th Int. Conf. on Rotor Dynamics – IFToMM, Springer, Mechanisms and Machine Science, Vol. 63, pp. 157-172, 2018.

[4] I. Nistor, P. Voinis, M. A. Hassini, R. Lacombe and P. Pennacchi, "Application of a Model Based Method for Balancing a Large Steam Turbo Generator Unit-page", Proc. of the 9th Int. Conf. on Rotor Dynamics-IFToMM, Springer, Mechanisms and Machine Science, Vol. 21, pp. 735-743, 2015.

[5] J. He and Z. Fu, Modal analysis, Butterworth-Heinemann, Oxford, England, 2001.

[6] M. I. Friswell, J. E. T. Penny, S. D. Garvey and A. W. Lees, Dynamics of Rotating Machines, Cambridge University Press, 2010.

[7] Yahya Muhammed Ameen and Jaafar Khalaf Ali, "Theoretical and experimental modal analysis of circular cross-section shaft", The Fourth Scientific Conference for Engineering and Postgraduate Research (PEc19), Baghdad, IOP Conference Series: Materials Science and Engineering, Vol. 745, No. 012066, 2019.

[8] J. M. Vance, B. Murphy and F. Zeidan, Machinery vibration and rotordynamics, John Wiley and Sons, 2010.

[9] R. Tiwari, Rotor Systems: Analysis and Identification, CRC Press, Boca Raton, 2017.

[10] Kreuzinger-Janik T., Irretier H., "Experimental Modal Analysis – A Tool for Unbalance Identification of Rotating Machines", International Journal of Rotating Machinery, Vol. 6, Article ID 304015, 2000.

[11] Jei, Y. G. and Kim, Y. J. Modal testing theory of rotor-bearing systems, 1993.

[12] M. H. Sadeghi, Soheil Jafari, Bahman Nasseroleslami, "Modal analysis of a turbo-pump shaft: An innovative suspending method to improve the results", International Journal of Engineering Science, Vol. 19, No. 5-1, pp. 143-149, 2008.

[13] Carvalho V. N., Dourado A. D., Rende B. R., Cavalini Jr A. A., Steffen Jr V., "Experimental validation of a robust model-based balancing approach", Journal of Vibration and Control, Vol. 25, Issue 2, pp. 423-434, 2019.

[14] Xialun Yun, Xuesong Mei, Gedong Jiang, Zhenbang Hu, and Zunhao Zhang, "Investigation on a No Trial Weight Spray Online Dynamic Balancer", Shock and Vibration, Vol. 2018, Article ID 7021215, 2018.

[15] Benjamin Siegl, and Richard Markert, "Model-based Non-stationary Unbalance Identification", 16th International Symposium on Transport Phenomena and Dynamics of Rotating Machinery, Honolulu, United States, Apr 2016.